The Effects of Activators on Zirconium Phosphinimide Ethylene Polymerization Catalysts

Emily Hollink, Pingrong Wei, and Douglas W. Stephan*

Department of Chemistry & Biochemistry, University of Windsor, Windsor, Ontario, Canada N9B 3P4

Received October 8, 2003

Synthetic routes to the species $CpZr(NPt\text{-}Bu_3)_2Cl$, **7**, $Cp_2Zr(NPt\text{-}Bu_3)Cl$, **8**, $CpZr(NPt\text{-}Bu_3)_2Me$, **9**, $Cp_2Zr(NPt\text{-}Bu_3)Me$, **10**, and $CpZr(NPt\text{-}Bu_3)_2Bn$, **11**, were developed in a manner similar to that previously reported for zirconium phosphinimide complexes. Rather than employing metathesis routes, transamination was considered to synthesize bis-phosphinimide zirconium complexes. At ambient temperature, $Zr(NPt\text{-}Bu_3)_3(NMe_2)$, **15**, was isolated in less than 5% yield, but could be obtained cleanly via reaction of $Zr(NPt\text{-}Bu_3)_3Cl$, **14**, with $LiNMe_2$. However, thermolysis of $Zr(NEt_2)_4$ with $HNPt\text{-}Bu_3$ afforded $Zr(NPt\text{-}Bu_3)_2(NEt_2)_2$, **12**, which was subsequently converted to $Zr(NPt\text{-}Bu_3)_2Cl_2$, **13**, upon reaction with trimethylsilyl chloride. Cationic products were generated from the reaction of Lewis acids in the presence of a donor to provide the salts $[CpZr(NPt\text{-}Bu_3)Me(THF)][MeB(C_6F_5)_3]$, **16**, $[Cp^*Zr(NPt\text{-}Bu_3)((i\text{-}PrN)_2CMe)][MeB(C_6F_5)_3]$, **17**, and $[CpZr(NPt\text{-}Bu_3)((i\text{-}PrN)_2CMe)][MeB(C_6F_5)_3]$, **18**. Similarly, reaction of $[HNMe_2Ph][B(C_6F_5)_4]$ with **4** generated the salt $[CpZr(NPt\text{-}Bu_3)Me(NMe_2Ph)][B(C_6F_5)_4]$, **19,** while reaction of **11** with $B(C_6F_5)_3$ gave the base-free product $[CpZr(NPt\text{-}Bu_3)_2][BnB(C_6F_5)_3]$, **20**. Structural considerations and preliminary MO calculations support the reactivity studies that augur well for olefin polymerization activity. Experimentally, previously reported screening using MAO as a solvent scrubber/activator with **1**−**4** showed only moderate polymerization activities. However, use of 20 equiv of $Al(i\text{-}Bu)_3$ as scavenger and 2 equiv of $B(C_6F_5)_3$ as cocatalyst resulted in a significant increase in activity relative to that observed upon activation with MAO. Use of $[Ph_3C][B(C_6F_5)_4]$ as the cocatalyst led to even higher ethylene polymerization activities.

Introduction

The research and development of post-metallocene homogeneous single-site olefin polymerization catalysts derived from group IV metal complexes has been the subject of intense efforts over the past two decades.[1−3] Of the systems that have been commercialized, the best known metallocene-type catalyst is the "constrained geometry catalyst" which is Ti-based.[4] Similarly, McConville and co-workers showed that Ti complexes of the chelating diamide ligand of the form $Ti(CH_2(CH_2NAr)_2))X_2$ ($Ar = (2,6\text{-}i\text{-}Pr_2)C_6H_3$, $(2,6\text{-}Me_2)C_6H_3$; X = Cl, Me) were highly active, living polymerization catalysts for α-olefins.[5−7] Schrock et al. described the species $Ti((t\text{-}Bu\text{-}d_6\text{-}N\text{-}o\text{-}C_6H_4)_2O)Me_2$, which upon activation by $[HNMe_2Ph][B(C_6F_5)_4]$, was inactive for olefin polymerization, while the Zr analogue effected living polymerization of 1-hexene.[8] More recently, Mitsui and researchers have reported a series of complexes of the general formula ML_2Cl_2 (M = Ti, Zr; L = salicylaldehyde derivative) that polymerize ethylene with extremely high turnover frequencies (>20 000 min^{-1} atm^{-1}) upon activation by MAO.[9−12] In our own work, we have furthered the development of ethylene polymerization catalysts by using Ti-phosphinimide complexes.[13−15] We have previously reported that several Zr-phosphinimide precursors, upon activation with MAO or $B(C_6F_5)_3$, exhibited relatively low polymerization activities.[16] In the former case, this was attributed to a catalyst deactivation pathway involving C−H bond activation derived from model reactions with $AlMe_3$ that afforded

* Corresponding author. E-mail: stephan@uwindsor.ca.

(1) Gibson, V. C.; Spitzmesser, S. K. *Chem. Rev.* **2003**, *103*, 283−315.
(2) Coates, G. W. *J. Chem. Soc. Dalton Trans.* **2002**, 467−475.
(3) Coates, G. W.; Hustad, P. D.; Reinartz, S. *Angew. Chem., Int. Ed.* **2002**, *41*, 2236−2257.
(4) Devore, D. D.; Timmers, F. J.; Hasha, D. L.; Rosen, R. K.; Marks, T. J.; Deck, P. A.; Stern, C. L. *Organometallics* **1995**, *14*, 3132−3134.
(5) Scollard, J. D.; McConville, D. H.; Rettig, S. J. *Organometallics* **1997**, *16*, 1810−1812.
(6) Guerin, F.; McConville, D. H.; Payne, N. C. *Organometallics* **1996**, *15*, 5085−5089.
(7) Scollard, J. D.; McConville, D. H.; Vittal, J. J.; Payne, N. C. *J. Mol. Catal. A* **1998**, *128*, 201−214.
(8) Schrock, R. R.; Baumann, R.; Reid, S. M.; Goodman, J. T.; Stumpf, R.; Davis, W. M. *Organometallics* **1999**, *18*, 3649−3670.
(9) Saito, J.; Mitani, M.; Mohri, J.-I.; Yoshida, Y.; Matsui, S.; Ishii, S.-I.; Kojoh, S.-I.; Kashiwa, N.; Fujita, T. *Angew. Chem., Int. Ed.* **2001**, *40*, 2918−2920.
(10) Mitani, M.; Mohri, J.; Yoshida, Y.; Saito, J.; Ishii, S.; Tsuru, K.; Matsui, S.; Furuyama, R.; Nakano, T.; Tanaka, H.; Kojoh, S.-i.; Matsugi, T.; Kashiwa, N.; Fujita, T. *J. Am. Chem. Soc.* **2002**, *124*, 3327−3336.
(11) Matsui, S.; Spaniol, T. P.; Takagi, Y.; Yoshida, Y.; Okuda, J. *J. Chem. Soc., Dalton Trans.* **2002**, 4529−4531.
(12) Matsui, S.; Fujita, T. *Catal. Today* **2001**, *66*, 63−73.
(13) Stephan, D. W.; Guerin, F.; Spence, R. E. v. H.; Koch, L.; Gao, X.; Brown, S. J.; Swabey, J. W.; Wang, Q.; Xu, W.; Zoricak, P.; Harrison, D. G. *Organometallics* **1999**, *18*, 2046−2048.
(14) Stephan, D. W.; Stewart, J. C.; Guerin, F.; Spence, R. E. v. H.; Xu, W.; Harrison, D. G. *Organometallics* **1999**, *18*, 1116−1118.
(15) Stephan, D. W.; Stewart, J. C.; Guerin, F.; Courtenay, S.; Kickham, J.; Hollink, E.; Beddie, C.; Hoskin, A.; Graham, T.; Wei, P.; Spence, R. E. v. H.; Xu, W.; Koch, L.; Gao, X.; Harrison, D. G. *Organometallics* **2003**, *22*, 1937−1947.
(16) Yue, N.; Hollink, E.; Guerin, F.; Stephan, D. W. *Organometallics* **2001**, *20*, 4424−4433.

10.1021/om030631c CCC: $27.50
Publication on Web 02/21/2004

Zr-methine clusters, including $(Cp^*Zr)_4(\mu\text{-}Cl)_5(Cl)(\mu\text{-}CH)_2$ and $(Cp^*Zr)_5(\mu\text{-}Cl)_6(\mu\text{-}CH)_3$. In the case of the borane activator $B(C_6F_5)_3$, stoichiometric reaction with $CpZr(NPt\text{-}Bu_3)Me_2$ effected methyl for aryl-group exchange, yielding the catalytically inactive product $CpZr(NPt\text{-}Bu_3)(C_6F_5)_2$. Despite these apparent deactivation pathways, computational models suggest that Zr-phosphinimide catalysts should be highly active as a result of a low barrier of ethylene insertion.[17] In this paper, we probe the synthesis and catalytic properties of cationic Zr-phosphinimide complexes, in addition to investigating the effect of the activating reagent on olefin polymerization activity.

Experimental Section

General Data. The syntheses were performed employing an atmosphere of dry, oxygen-free nitrogen in a Vacuum Atmospheres inert atmosphere glovebox or standard Schlenk techniques. Solvents were purified employing Grubbs-type column systems manufactured by Innovative Technology. ^{1}H NMR data were acquired on a Bruker Avance 500 MHz spectrometer, and $^{13}C\{^1H\}$ and $^{31}P\{^1H\}$ NMR data on a Bruker Avance 300 MHz spectrometer. ^{1}H and ^{13}C NMR chemical shifts are listed downfield from $SiMe_4$ in parts per million and were referenced to the residual proton or carbon peak of the solvent. ^{31}P NMR data were referenced using an external standard relative to 85% H_3PO_4. All NMR spectra were recorded in C_6D_6 unless otherwise stated. Galbraith Laboratories Inc. or in-house EA services performed the combustion analyses. In several cases, despite repeated analyses and the use of added oxidant, C analyses yielded deviations from calculated values. We attribute this to partial formation of zirconium carbides during combustion of the organometallic derivatives. GPC analyses were performed employing a Waters 150C GPC using 1,2,4-trichlorobenzene as the mobile phase at 140 °C at NOVA Research and Technology Centre in Calgary. The samples were prepared by dissolving the polymer in the mobile phase solvent in an external oven at 0.1% (w/v) and were filtered before injection. Molecular weights are expressed as polyethylene equivalents with a relative standard deviation of 2.9% and 5.0% for the M_n and M_w respectively. Benzene, toluene, and Et_2O were dried over Na, MeOH was dried over Mg, and NEt_3 was dried over KOH prior to distillation. C_6D_6 and CD_2Cl_2 were purchased from Canadian Isotopes Laboratories and degassed by at least four freeze/pump/thaw cycles before storing over 4 Å molecular sieves. The compounds $Cp^*Zr(NPt\text{-}Bu_3)Cl_2$, **1**, $CpZr(NPt\text{-}Bu_3)Cl_2$, **2**, $Cp^*Zr(NPt\text{-}Bu_3)Me_2$, **3**, $CpZr(NPt\text{-}Bu_3)Me_2$, **4**, $Cp^*Zr(NPt\text{-}Bu_3)Bn_2$, **5**, and $CpZr(NPt\text{-}Bu_3)Bn_2$, **6**, were prepared according to literature methods.[16]

Synthesis of $CpZr(NPt\text{-}Bu_3)_2Cl$, 7. Solid $LiNPt\text{-}Bu_3$ (160 mg, 0.72 mmol) was added in several portions over a 30 min period to a slurry of $[ZrCpCl_3]_n$ (180 mg, 0.72 mmol) in benzene (20 mL). The mixture was stirred for 48 h at 25 °C, after which time it was filtered through a Hyflo Super Cel. Gradual removal of the solvent in vacuo afforded colorless crystals (260 mg, 81%). ^{1}H NMR δ: 6.57 (s, 5H, Cp), 1.27 (d, 54H, $^3J_{P-H}$ = 5 Hz, *t*-Bu). $^{13}C\{^1H\}$ NMR δ: 110.6 (s, Cp), 40.6 (d, $^1J_{P-C}$ = 48 Hz, *t*-Bu), 29.9 (s, *t*-Bu). $^{31}P\{^1H\}$ NMR δ: 31.5 (s). Anal. Calcd for $C_{29}H_{59}ClN_2P_2Zr$: C, 55.78; H, 9.52; N, 4.49. Found: C, 55.65; H, 9.80; N, 4.52.

Synthesis of $Cp_2Zr(NPt\text{-}Bu_3)Cl$, 8. $ZrCp_2HCl$ (320 mg, 1.2 mmol) was slurried in benzene (35 mL), and a suspension of $HNPt\text{-}Bu_3$ (270 mg, 1.2 mmol) in the same solvent (5 mL) was added dropwise at 25 °C. The mixture was stirred for 12 h, after which time the solvent was gradually removed in vacuo, affording colorless crystals (520 mg, 92%). ^{1}H NMR δ: 6.19 (s, 10H, Cp), 1.16 (d, 27H, $^3J_{P-H}$ = 13 Hz, *t*-Bu). $^{13}C\{^1H\}$ NMR δ: 112.5 (s, Cp), 40.8 (d, $^1J_{P-C}$ = 47 Hz, *t*-Bu), 29.9 (s, *t*-Bu). $^{31}P\{^1H\}$ NMR δ: 36.4 (s). Anal. Calcd for $C_{22}H_{37}ClNPZr$: C, 55.84; H, 7.88; N, 2.96. Found: C, 55.40; H, 7.61; N, 2.86. Colorless crystals suitable for X-ray diffraction were grown by slow evaporation from benzene.

Synthesis of $CpZr(NPt\text{-}Bu_3)_2Me$, 9, $Cp_2Zr(NPt\text{-}Bu_3)Me$, 10, and $CpZr(NPt\text{-}Bu_3)_2Bn$, 11. These compounds were prepared in a similar fashion using the appropriate Grignard reagent, and thus only one preparation is detailed. A 3.0 M solution of MeMgBr in Et_2O (3.6 mmol) was added dropwise at 25 °C to a slurry of **7** (320 mg, 0.72 mmol) in the same solvent (30 mL). The heterogeneous mixture was stirred for 15 h, after which time the solvent was removed in vacuo. The product was extracted with hexanes (3 × 20 mL), and the extracts were filtered through a Hyflo Super Cel. Removal of the solvent afforded a white solid (210 mg, 72%). **9**: Yield: 235 mg, 85%. ^{1}H NMR δ: 6.41 (s, 5H, Cp), 1.27 (d, 54H, $^3J_{P-H}$ = 12 Hz, *t*-Bu), 0.33 (s, 3H, Me). $^{13}C\{^1H\}$ NMR δ: 108.9 (s, Cp), 40.4 (d, $^1J_{P-C}$ = 48 Hz, *t*-Bu), 30.0 (s, *t*-Bu), 29.5 (s, Me). $^{31}P\{^1H\}$ NMR δ: 28.5 (s). Anal. Calcd for $C_{30}H_{62}N_2P_2Zr$: C, 59.66; H, 10.35; N, 4.64. Found: C, 54.24; H, 9.86; N, 4.38. **10**: colorless crystals. Yield: 112 mg, 82%. ^{1}H NMR δ: 5.97 (s, 10H, Cp), 1.13 (d, 27H, $^3J_{P-H}$ = 12 Hz, *t*-Bu), 0.39 (s, 3H, Me). $^{13}C\{^1H\}$ NMR δ: 109.5 (s, Cp), 40.5 (d, $^1J_{P-C}$ = 28 Hz, *t*-Bu), 29.9 (s, *t*-Bu), 16.6 (s, Me). $^{31}P\{^1H\}$ NMR δ: 33.0 (s). Calcd for $C_{23}H_{40}NPZr$: C, 61.01; H, 8.90; N, 3.09. Found: C, 60.51; H, 8.96; N, 2.95. **11**: Yield: 156 mg, 89%. ^{1}H NMR δ: 7.38 (d, 2H, $^3J_{H-H}$ = 7 Hz, Ph (*o*-H)), 7.33 (t, 2H, $^3J_{H-H}$ = 7 Hz, Ph (*m*-H)), 6.93 (t, 1H, $^3J_{H-H}$ = 7 Hz, Ph (*p*-H)), 6.30 (s, 5H, Cp), 2.69 (s, 2H, CH_2), 1.27 (d, 54H, $^3J_{P-H}$ = 12 Hz, *t*-Bu). $^{13}C\{^1H\}$ NMR δ: 155.5 (s, Ph (ipso-C)), 126.2 (s, Ph (*o*-C)), 124.3 (s, Ph (*m*-C)), 119.0 (s, Ph (*p*-C)), 110.2 (s, Cp), 47.1 (s, CH_2), 40.4 (d, $^1J_{P-C}$ = 47 Hz, *t*-Bu), 30.0 (s, *t*-Bu). $^{31}P\{^1H\}$ NMR δ: 29.7 (s). Anal. Calcd for $C_{36}H_{66}N_2P_2Zr$: C, 63.58; H, 9.78; N, 4.12. Found: C, 63.99; H, 9.38; N, 4.09. Colorless crystals suitable for X-ray diffraction were grown by slow evaporation from hexanes.

Synthesis of $Zr(NPt\text{-}Bu_3)_2(NEt_2)_2$, 12. A suspension of $HNPt\text{-}Bu_3$ (890 mg, 4.0 mmol) in PhMe (20 mL) was added dropwise to a clear solution of $Zr(NEt_2)_4$ (777 mg, 2.0 mmol) in the same solvent (50 mL). The clear mixture was heated at reflux for 12 h, after which time the volatile products were removed in vacuo. The product was purified by recrystallization in pentane/Et_2O at −35 °C to afford colorless crystals of **12** (1.24 g, 93%). ^{1}H NMR δ: 3.72 (q, 8H, $^3J_{H-H}$ = 7 Hz, NCH_2), 1.36 (d, 54H, $^3J_{P-H}$ = 12 Hz, *t*-Bu), 1.31 (t, 12H, $^3J_{H-H}$ = 7 Hz, CH_2Me). $^{13}C\{^1H\}$ NMR δ: 44.7 (s, NCH_2), 40.2 (d, $^1J_{P-C}$ = 48 Hz, *t*-Bu), 30.1 (s, *t*-Bu), 16.6 (s, NCH_2Me). $^{31}P\{^1H\}$ NMR δ: 28.5 (s). Anal. Calcd for $C_{32}H_{74}N_4P_2Zr$: C, 57.53; H, 11.16; N, 8.39. Found: C, 57.16; H, 10.84; N, 8.10. Colorless crystals suitable for X-ray diffraction were grown by slow evaporation from pentane.

Synthesis of $Zr(NPt\text{-}Bu_3)_2Cl_2$, 13. Me_3SiCl (0.18 mL, 1.45 mmol) was added to a solution of **12** (464 mg, 0.69 mmol) in benzene (40 mL). The clear solution was stirred at 25 °C for 20 h, after which time the volatile products were removed in vacuo. The solid was washed with pentane (3 × 10 mL) and dried to afford a white solid (332 mg, 81%). ^{1}H NMR δ: 1.29 (d, 54H, $^3J_{P-H}$ = 13 Hz, *t*-Bu). $^{13}C\{^1H\}$ NMR δ: 40.5 (d, $^1J_{P-C}$ = 47 Hz, *t*-Bu), 29.7 (s, *t*-Bu). $^{31}P\{^1H\}$ NMR δ: 35.6 (s). Anal. Calcd for $C_{24}H_{54}Cl_2N_2P_2Zr$: C, 48.46; H, 9.15; N, 4.71. Found: C, 48.02; H, 9.51; N, 4.62.

Synthesis of $Zr(NPt\text{-}Bu_3)_3Cl$, 14. An improved synthesis for this previously reported compound is described.[16] Solid $ZrCl_4$ (183 mg, 0.79 mmol) was dissolved in THF (15 mL) at −35 °C, and a clear solution of $LiNPt\text{-}Bu_3$ (527 mg, 2.36 mmol) in the same solvent (10 mL) was added dropwise over a 10 min period. The solution was warmed to 25 °C and stirred for 12 h, during which time the yellow color disappeared. The solvent was removed in vacuo, and the product was extracted with benzene (2 × 15 mL). Following filtration through a Hyflo Super Cel, the solvent was removed in vacuo, affording a white

(17) Vanka, K.; Xu, Z.; Ziegler, T. *Isr. J. Chem.* **2003**, *42*, 403−415.

solid. Analytically pure product was obtained by recrystallizing the crude mixture from toluene/pentane at −35 °C to ultimately afford colorless crystals (238 mg, 39%). The spectroscopic data agreed with literature values.[16]

Synthesis of Zr(NP*t*-Bu$_3$)$_3$(NMe$_2$), 15. The compound **14** (201 mg, 0.26 mmol) was dissolved in benzene (20 mL), and solid $LiNMe_2$ (41 mg, 0.79 mmol) was added at 25 °C. The mixture was stirred for 20 h, after which time it was filtered through a Hyflo Super Cel. The solvent was removed in vacuo to afford a white solid (124 mg, 61%). ^{1}H NMR δ: 3.53 (s, 6H, NMe_2), 1.45 (s, 81H, $^3J_{P-H}$ = 12 Hz, *t*-Bu). ^{13}C{^{1}H} NMR δ: 46.9 (s, NMe_2), 40.2 (d, $^1J_{P-C}$ = 48 Hz, *t*-Bu), 30.4 (s, *t*-Bu). ^{31}P{^{1}H} NMR δ: 26.1 (s). Anal. Calcd for $C_{38}H_{87}N_4P_3Zr$: C, 58.20; H, 11.18; N, 7.14. Found: C, 58.21; H, 11.08; N, 7.26. Colorless crystals suitable for X-ray diffraction were grown by slow evaporation from pentane.

Generation of [CpZr(NP*t*-Bu$_3$)Me(THF)][MeB(C$_6$F$_5$)$_3$], 16, and [CpZr(NP*t*-Bu$_3$)Me(NMe$_2$Ph)][B(C$_6$F$_5$)$_4$], 19. These compounds were prepared via reactions similar to that of **4** with $B(C_6F_5)_3$ in the presence of 10 equiv of THF or [NMe_2HPh][$B(C_6F_5)_4$], respectively; thus one preparation is detailed. Compound **4** (24 mg, 0.060 mmol) and $B(C_6F_5)_3$ (31 mg, 0.060 mmol) were dissolved in 1 mL (each) of CH_2Cl_2 to give clear, colorless solutions. THF (50 μL, 0.60 mmol) if required was added at 25 °C to the solution containing the Zr precursor, followed immediately by the solution of $B(C_6F_5)_3$. The pale yellow mixture was stirred for 30 min, then the solvents were removed in vacuo. The residue was washed with pentane (2 × 2 mL) and dried in vacuo to afford a pale yellow solid (46 mg, 78%). In both cases, the products formed quantitatively, as indicated by NMR spectroscopy; however due the sensitive nature of the products, satisfactory microanalyses were not obtained. **16**: ^{1}H NMR (CD_2Cl_2) δ: 6.51 (s, 5H, Cp), 4.02 (br, 4H, OCH_2), 2.05 (br, 4H, CH_2CH_2), 1.45 (d, 27H, $^3J_{P-H}$ = 13 Hz, *t*-Bu), 0.50 (s, 3H, ZrMe), 0.49 (br s, 3H, MeB). ^{13}C{^{1}H} NMR (CD_2Cl_2) δ: 149.7 (br s, C_6F_5 (ipso)), 148.7 (d(br), $^1J_{C-F}$ = 240 Hz, C_6F_5 (*o*-C)), 138.8 (d(m), $^1J_{C-F}$ = 245 Hz, C_6F_5 (*p*-C)), 136.9 (d(m), $^1J_{C-F}$ = 240 Hz, C_6F_5 (*m*-C)), 113.6 (s, Cp), 73.9 (s, OCH_2), 41.2 (d, $^1J_{P-C}$ = 45 Hz, *t*-Bu), 30.3 (s, *t*-Bu), 29.0 (ZrMe), 26.1 (s, CH_2CH_2), 12.5 (br q, J_{B-C} = 20 Hz, MeB). ^{11}B{^{1}H} NMR (CD_2Cl_2) δ: −20.8 (s). ^{19}F{^{1}H} NMR (CD_2Cl_2) δ: −132.92 (d, 6F, $^3J_{F-F}$ = 8 Hz, C_6F_5 (*o*-F)), −163.98 (t, 3F, $^3J_{F-F}$ = 20 Hz, C_6F_5 (*p*-F)), −167.80 (m, 6F, C_6F_5 (*m*-F)). ^{31}P{^{1}H} NMR (CD_2Cl_2) δ: 46.6 (s). **19**: ^{1}H NMR (CD_2Cl_2) δ: 7.69 (t, 2H, $^3J_{H-H}$ = 8 Hz, Ph (*m*-H)), 7.62 (t, 1H, $^3J_{H-H}$ = 8 Hz, Ph (*p*-H)), 7.48 (d, 2H, $^3J_{H-H}$ = 8 Hz, Ph (*o*-H)), 5.87 (s, 5H, Cp), 3.20 (s, 3H, NMe), 3.03 (s, 3H, NMe), 1.50 (d, 27H, $^3J_{P-H}$ = 13 Hz, *t*-Bu), 0.62 (s, 3H, ZrMe). ^{13}C{^{1}H} NMR (CD_2Cl_2) δ: 148.4 (d(br), $^1J_{C-F}$ = 240 Hz, C_6F_5 (*o*-C)), 141.0 (s, C_6F_5, (ipso-C)), 138.4 (d(br), $^1J_{C-F}$ = 249 Hz, C_6F_5 (*p*-C)), 136.5 (d(br), $^1J_{C-F}$ = 244 Hz, C_6F_5 (*m*-C)), 133.2 (s, Ph (*m*-C)), 129.7 (s, Ph (*p*-C)), 129.2 (s, Ph (ipso-C)), 117.6 (s, Ph (*o*-C)), 113.3 (s, Cp), 51.0 (s, NMe), 45.8 (s, NMe), 33.9 (s, ZrMe), 41.2 (d, $^1J_{P-C}$ = 45 Hz, *t*-Bu), 29.6 (s, *t*-Bu). ^{11}B{^{1}H} NMR (CD_2Cl_2) δ: −16.9 (s). ^{19}F{^{1}H} NMR (CD_2Cl_2) δ: −133.32 (d, 8F, $^3J_{F-F}$ = 8 Hz, C_6F_5 (*o*-F)), −163.93 (t, 4F, $^3J_{F-F}$ = 20 Hz, C_6F_5 (*p*-F)), −167.76 (pseudo t, 8F, $^3J_{F-F}$ = 20 Hz, C_6F_5 (*m*-F)). ^{31}P{^{1}H} NMR (CD_2Cl_2) δ: 47.2 (s).

Synthesis of [Cp*Zr(NP*t*-Bu$_3$)((*i*-PrN)$_2$CMe)][MeB(C$_6$F$_5$)$_3$], 17, and [CpZr(NP*t*-Bu$_3$)((*i*-PrN)$_2$CMe)][MeB(C$_6$F$_5$)$_3$], 18. These compounds were prepared in a similar fashion, and thus only one preparation is detailed. Compound **3** (99 mg, 0.24 mmol) and (*i*-PrN)$_2$C (40 μL, 0.24 mmol) were combined in benzene (5 mL) to give a colorless solution. A clear solution of $B(C_6F_5)_3$ (126 mg, 0.24 mmol) in the same solvent (5 mL) was added at 25 °C, and a bright yellow oil separated immediately. After stirring for 5 min, the organic layer was pipetted off, and the oil was washed with benzene (3 × 3 mL) and pentane (3 × 3 mL). Drying in vacuo resulted in a bright yellow solid (132 mg, 53%). **17**: Yield: 72 mg, 77%. ^{1}H NMR (CD_2Cl_2) δ: 3.74 (s, 2H, $^3J_{H-H}$ = 6 Hz, *i*-Pr), 2.22 (s, 3H, NCMe), 2.21 (s, 15H, Cp*), 1.37 (d, 27H, $^3J_{P-H}$ = 13 Hz, *t*-Bu), 1.23 (d, 6H, $^3J_{H-H}$ = 6 Hz, *i*-Pr), 1.15 (d, 6H, $^3J_{H-H}$ = 6 Hz, *i*-Pr), 0.50 (br s, 3H, MeB). ^{13}C{^{1}H} NMR (CD_2Cl_2) δ: 172.7 (s, NCMe), 148.9 (dd, $^1J_{C-F}$ = 235 Hz, $^2J_{C-F}$ = 11 Hz, C_6F_5 (*o*-C)), 138.0 (d(m), $^1J_{C-F}$ = 240 Hz, C_6F_5 (*p*-C)), 136.9 (ddd, $^1J_{C-F}$ = 245 Hz,$^2J_{C-F}$ = 22 Hz, $^3J_{C-F}$ = 12 Hz, C_6F_5 (*m*-C)), 128.9 (br s, C_6F_5 (ipso)), 125.7 (s, Cp*), 49.4 (s, *i*-Pr), 40.7 (d, $^1J_{P-C}$ = 45 Hz, *t*-Bu), 29.7 (s, *t*-Bu), 25.7 (s, *i*-Pr), 25.6 (s, *i*-Pr), 14.6 (s, NCMe), 12.8 (s, Cp*), 10.5 (br q, J_{B-C} = 50 Hz, MeB). ^{11}B{^{1}H} NMR (CD_2Cl_2) δ: −19.1 (s). ^{19}F{^{1}H} NMR (CD_2Cl_2) δ: −133.40 (d, 6F, $^3J_{F-F}$ = 20 Hz, C_6F_5 (*o*-F)), −165.64 (t, 3F, $^3J_{F-F}$ = 20 Hz, C_6F_5 (*p*-F)), −168.17 (m, 6F, C_6F_5 (*m*-F)). ^{31}P{^{1}H} NMR (CD_2Cl_2) δ: 47.2 (s). Anal. Calcd for $C_{49}H_{62}BF_{15}N_3PZr$: C, 52.97; H, 5.62; N, 3.78. Found: C, 52.69; H, 5.82; N, 3.79. **18**: ^{1}H NMR (CD_2Cl_2) δ: 6.71 (s, 5H, Cp), 3.79 (sept, 2H, $^3J_{H-H}$ = 6 Hz, *i*-Pr), 2.19 (s, 3H, NCMe), 1.39 (d, 27H, $^3J_{P-H}$ = 7 Hz, *t*-Bu), 1.19 (d, 6H, $^3J_{H-H}$ = 6 Hz, *i*-Pr), 1.11 (d, 6H, $^3J_{H-H}$ = 6 Hz, *i*-Pr), 0.52 (br s, 3H, MeB). ^{13}C{^{1}H} NMR (CD_2Cl_2) δ: 170.7 (s, NCMe), 148.9 (dd, $^1J_{C-F}$ = 235 Hz, $^2J_{C-F}$ = 10 Hz, C_6F_5 (*o*-C)), 138.1 (d(m), $^1J_{C-F}$ = 240 Hz, C_6F_5 (*p*-C)), 136.9 (ddd, $^1J_{C-F}$ = 250 Hz,$^2J_{C-F}$ = 20 Hz, $^3J_{C-F}$ = 11 Hz, C_6F_5 (*m*-C)), 129.6 (br s, C_6F_5 (ipso)), 115.6 (s, Cp), 49.5 (s, *i*-Pr), 40.8 (d, $^1J_{P-C}$ = 60 Hz, *t*-Bu), 29.7 (s, *t*-Bu), 26.2 (s, *i*-Pr), 25.5 (s, *i*-Pr), 13.7 (s, NCMe), 10.6 (br q, J_{B-C} = 52 Hz, MeB). ^{11}B{^{1}H} NMR (CD_2Cl_2) δ: −19.1 (s). ^{19}F{^{1}H} NMR (CD_2Cl_2) δ: −133.27 (d, 6F, $^3J_{F-F}$ = 20 Hz, C_6F_5 (*o*-F)), −163.54 (t, 3F, $^3J_{F-F}$ = 20 Hz, C_6F_5 (*p*-F)), −168.03 (m, 6F, C_6F_5 (*m*-F)). ^{31}P{^{1}H} NMR (CD_2Cl_2) δ: 46.5 (s). Anal. Calcd for $C_{44}H_{52}BF_{15}N_3PZr$: C, 50.77; H, 5.04; N, 4.04. Found: C, 50.42; H, 5.19; N, 4.17.

Generation of [CpZr(NP*t*-Bu$_3$)$_2$][BnB(C$_6$F$_5$)$_3$], 20. Solid **11** (51 mg, 0.075 mmol) and $B(C_6F_5)_3$ (38 mg, 0.075 mmol) were dissolved separately in benzene (2 mL each) to give clear solutions. They were combined at 25 °C, and a red insoluble oil separated immediately. The benzene layer was decanted off, and the oil was washed with benzene (3 × 1 mL) before drying in vacuo. Yield: 83 mg (93%). ^{1}H NMR (CD_2Cl_2) δ: 7.64 (br, 2H, Ph (*m*-H)), 7.45 (s, 1H, Ph (*p*-H)), 7.17 (br, 2H, Ph (*o*-H)), 6.81 (s, 5H, Cp), 3.42 (br, 2H, CH_2), 1.69 (d, 54H, $^3J_{P-H}$ = 13 Hz, *t*-Bu). ^{13}C{^{1}H} NMR (CD_2Cl_2) δ: 149.9 (s, C_6F_5, (ipso-C)), 149.3 (d(br), $^1J_{C-F}$ = 240 Hz, C_6F_5 (*o*-C)), 138.5 (d(br), $^1J_{C-F}$ = 240 Hz, C_6F_5 (*p*-C)), 137.5 (d(br), $^1J_{C-F}$ = 240 Hz, C_6F_5 (*m*-C)), 129.7 (s, Ph (ipso-C)), 129.8 (s, Ph (*o*-C)), 127.7 (s, Ph (*m*-C)), 123.3 (s, Ph (*p*-C)), 112.4 (s, Cp), 71.2 (s, CH_2), 40.9 (d, $^1J_{P-C}$ = 36 Hz, *t*-Bu), 30.6 (s, *t*-Bu). ^{11}B{^{1}H} NMR (CD_2Cl_2) δ: −16.6 (s). ^{19}F{^{1}H} NMR (CD_2Cl_2) δ: −131.14 (d, 6F, $^3J_{F-F}$ = 20 Hz, C_6F_5 (*o*-F)), −165.02 (t, 3F, $^3J_{F-F}$ = 20 Hz, C_6F_5 (*p*-F)), −167.71 (t, 6F, $^3J_{F-F}$ = 20 Hz, C_6F_5 (*m*-F)). ^{31}P{^{1}H} NMR (CD_2Cl_2) δ: 37.9 (s).

Polymerization Protocol. A 1 L Buchi reactor was dried in vacuo (10^{-2} mmHg) for several hours. Toluene (500 mL) was transferred into the vessel under a positive pressure of N_2 and was heated to 30 °C. The temperature was controlled (to ca. +2 °C) with an external heating/cooling bath and was monitored by a thermocouple that extended into the polymerization vessel. The vessel was vented of N_2 and then pressurized with C_2H_4 (12 psig), while the solvent stirred at a rate of 150 rpm. A solution of MAO (1000 equiv, 10% in toluene) was injected, and the mixture was stirred for 5 min. A solution of the precatalyst (toluene, 50 μmol) was injected, and the rate of stirring was increased to 1000 rpm, while the solution stirred for 30 min. Any recorded exotherm was within the allowed temperature differential of the heating/cooling system. The reaction was quenched by pouring the reaction mixture into a solution of 1 M HCl in MeOH. The precipitated polymer was subsequently washed with HCl, HCl/MeOH, and toluene before drying at 50 °C for at least 48 h prior to weighing.

Molecular Orbital Calculations. Single-point calculations were executed using Gaussian 98 software (revision A.11.1).[18] The initial *Z*-matrixes were derived from data obtained from crystallographic analyses of the compounds; all C−H bond

distances were modified to 1.089Å. The geometries were obtained using the Hartree−Fock method and STO-3g basis set. Graphical representations of the HOMO and LUMO orbitals were generated using Chem3D.

X-ray Data Collection and Reduction. Crystals were manipulated and mounted in capillaries in a glovebox, thus maintaining a dry, O_2-free environment for each crystal. Diffraction experiments were performed on a Siemens SMA25oC System CCD diffractometer. The data were collected in a hemisphere of data in 1329 frames with 10 s exposure times. The observed extinctions were consistent with the space groups in each case. The data sets were collected ($4.5° < 2\theta < 45-50.0°$). A measure of decay was obtained by re-collecting the first 50 frames of each data set. The intensities of reflections within these frames showed no statistically significant change over the duration of the data collections. The data were processed using the SAINT and XPREP processing packages. An empirical absorption correction based on redundant data was applied to each data set. Subsequent solution and refinement was performed using the SHELXTL solution package operating on a Pentium computer.

Structure Solution and Refinement. Non-hydrogen atomic scattering factors were taken from the literature tabulations.[19] The heavy atom positions were determined using direct methods employing the SHELXTL direct methods routine. The remaining non-hydrogen atoms were located from successive difference Fourier map calculations. The refinements were carried out by using full-matrix least-squares techniques on F, minimizing the function $w(|F_o| - |F_c|)^2$ where the weight w is defined as $4F_o^2/2\sigma(F_o^2)$ and F_o and F_c are the observed and calculated structure factor amplitudes. In the final cycles of each refinement, all non-hydrogen atoms were assigned anisotropic temperature factors in the absence of disorder or insufficient data. In the latter cases atoms were treated isotropically. C−H atom positions were calculated and allowed to ride on the carbon to which they are bonded assuming a C−H bond length of 0.95 Å. H atom temperature factors were fixed at 1.10 times the isotropic temperature factor of the C atom to which they are bonded. The H atom contributions were calculated, but not refined. The locations of the largest peaks in the final difference Fourier map calculation as well as the magnitude of the residual electron densities in each case were of no chemical significance. Additional details are provided in the Supporting Information.

Results and Discussion

Synthetic routes to Zr-phosphinimides have been investigated to a limited extent. We have previously reported the synthesis of the species Cp*Zr(NP*t*-Bu$_3$)Cl$_2$, **1**, CpZr(NP*t*-Bu$_3$)Cl$_2$, **2**, Cp*Zr(NP*t*-Bu$_3$)Me$_2$, **3**, CpZr(NP*t*-Bu$_3$)Me$_2$, **4**, Cp*Zr(NP*t*-Bu$_3$)Bn$_2$, **5**, and CpZr(NP*t*-Bu$_3$)Bn$_2$, **6**, and have performed a preliminary evaluation of their utility as olefin polymerization catalysts.[16] In a similar fashion, the synthetic methodology has been extended to prepare the related species CpZr(NP*t*-Bu$_3$)$_2$Cl, **7**, from the reaction of $[CpZrCl_3]_n$ with 2 equiv of the phosphinimide salt. In addition, a reliable synthesis of the species Cp$_2$Zr(NP*t*-Bu$_3$)Cl, **8**, was developed on the basis of the reaction of Schwartz's reagent, Cp$_2$ZrHCl, with HNP*t*-Bu$_3$. The X-ray structures of **1** and **8**, not previously reported, were also determined (Figure 1). In addition, preliminary X-ray data for **7** were also obtained. The geometries of **1** and **8** were as expected with Zr−N distances of 1.923(2) and 1.978(5) Å and P−N−Zr angles of 163.49(12)° and 171.9(3)°, respectively. The slightly shorter Zr−N distance in **1** is consistent with the presence of the two η^5-cyclopentadienyl rings in **8**, as both steric crowding and the relatively electron-rich Zr center in **8** result in a longer Zr−N bond. The Zr−N bond length and P−N−Zr angle in **1** are similar to those previously reported for **2** (1.902(5) Å, 174.8(4)°) and Cp*Zr(NP*i*-Pr$_3$)Cl$_2$ (1.926(7) Å, 175.2(4)°).[16]

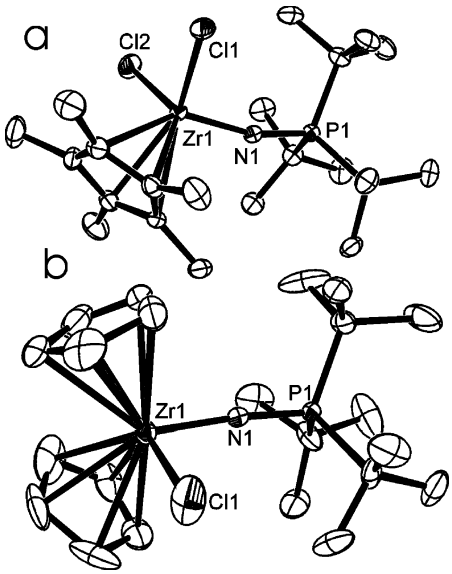

Figure 1. ORTEP drawings of (a) **1** and (b) **8**, with 30% thermal ellipsoids. Hydrogen atoms are omitted for clarity. Distances (Å) angles (deg): (a) Zr(1)−N(1) 1.923(2), Zr(1)−Cl(2) 2.4311(10), Zr(1)−Cl(1) 2.4423(11), P(1)−N(1) 1.593(2), N(1)−Zr(1)−Cl(2) 104.20(7), N(1)−Zr(1)−Cl(1) 103.72(7), Cl(2)−Zr(1)−Cl(1) 104.46(4), P(1)−N(1)−Zr(1) 163.49(12); (b) Zr(1)−N(1) 1.978(5), Zr(1)−Cl(1) 2.511(3), P(1)−N(1) 1.583(5), N(1)−Zr(1)−Cl(1) 96.91(17), P(1)−N(1)−Zr(1) 171.9(3).

Alkylation with Grignard reagents was previously used to prepare Cp*Zr(NP*t*-Bu$_3$)Me$_2$, **3**, CpZr(NP*t*-Bu$_3$)Me$_2$, **4**, Cp*Zr(NP*t*-Bu$_3$)Bn$_2$, **5**, and CpZr(NP*t*-Bu$_3$)Bn$_2$, **6**, in reasonable yields.[16] In a similar fashion, the species CpZr(NP*t*-Bu$_3$)$_2$Me, **9**, Cp$_2$Zr(NP*t*-Bu$_3$)Me, **10**, and CpZr(NP*t*-Bu$_3$)$_2$Bn, **11**, were prepared from the appropriate chloride precursors. The compounds **6** and **11** were characterized by X-ray methods (Figures 2, 3). The structure of **6** suggests an η^2-Zr−benzyl interaction as evidenced by the Zr−C(25) distance of 2.335(3) Å and the Zr−C$_{ipso}$ close approach of 2.779(3) Å. The corresponding Zr−C−C$_{ipso}$ angle is 90.93(18)°.[20] Similar η^2-interactions have been reported in the compounds Zr(O-2,6-*t*-Bu$_2$C$_6$H$_3$)Bn$_3$,[21] Zr(C$_5$H$_4$(RMe$_2$CH$_2$Ph))Bn$_3$ (R = C,[22] Si[23]), Zr(CH$_2$C$_6$H$_4$*p*-*t*-Bu)$_4$,[24] and Cp*HfBn$_3$.[25] The Zr−N distance of 1.951(2) Å and the Zr−N−P angle of 171.84(13)° are similar to those seen in dichloride analogues above. ^{1}H NMR evidence indicates that the

(18) Frisch, M. J.; Trucks, G. W.; Schlegel, H. B.; Scuseria, G. E.; Robb, M. A.; Cheeseman, J. R.; Zakrzewski, V. G.; Montgomery, J. A. J.; Stratmann, R. E.; Burant, J. C.; Dapprich, S.; Millam, J. M.; Daniels, A. D. K., K. N.; Strain, M. C.; Farkas, O.; Tomasi, J.; Barone, V.; Cossi, M.; Cammi, R.; Mennucci, B.; Pomelli, C.; Adamo, C.; Clifford, S.; Ochterski, J.; Petersson, G. A.; Ayala, P. Y.; Cui, Q.; Morokuma, K.; Salvador, P.; Dannenberg, J. J.; Malick, D. K.; Rabuck, A. D.; Raghavachari, K.; Foresman, J. B.; Cioslowski, J.; Ortiz, J. V.; Baboul, A. G.; Stefanov, B. B.; Liu, G.; Liashenko, A.; Piskorz, P.; Komaromi, I.; Gomperts, R.; Martin, R. L.; Fox, D. J.; Keith, T.; Al-Laham, M. A.; Peng, C. Y.; Nanayakkara, A.; Challacombe, M.; Gill, P. M. W.; Johnson, B.; Chen, W.; Wong, M. W.; Andres, J. L.; Gonzalez, C.; Head-Gordon, M.; Replogle, E. S.; Pople, J. A. *Gaussian 98* (revision A.11.1); Gaussian, Inc.: Pittsburgh, PA, 2001.

(19) Cromer, D. T.; Mann, J. B. *Acta Crystallogr. A* **1968**, *A24*, 321−324.

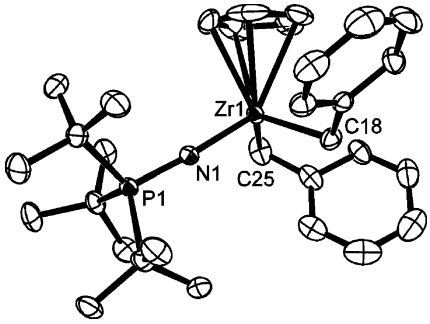

Figure 2. ORTEP drawing of **6**, with 30% thermal ellipsoids. Hydrogen atoms are omitted for clarity. Distances (Å) angles (deg): Zr(1)−N(1) 1.951(2), Zr(1)−C(18) 2.330(3), Zr(1)−C(25) 2.335(3), Zr(1)−C(26) 2.779(3), P(1)−N(1) 1.592(2), N(1)−Zr(1)−C(18) 102.23(10), N(1)−Zr(1)−C(25) 101.78(11), C(18)−Zr(1)−C(25) 117.24(11), N(1)−Zr(1)−C(26) 111.52(9), C(18)−Zr(1)−C(26) 85.32(9), C(25)−Zr(1)−C(26) 31.93(11), P(1)−N(1)−Zr(1) 171.84(13).

Scheme 1

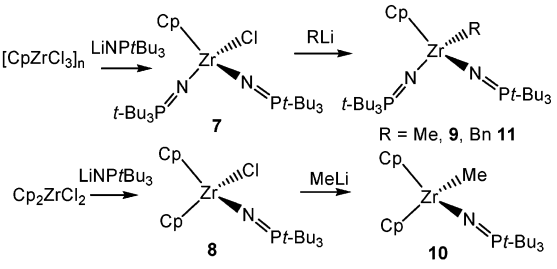

η^2-interactions do not persist in solution, suggesting that this phenomenon is due to crystal-packing forces rather than an unusually electrophilic metal center.[20] In contrast to **6**, X-ray analysis of **11** revealed an η^1-coordinated Zr−benzyl interaction with a Zr−C distance of 2.322(3) Å. The Zr−N distances and P−N−Zr angles were typical.

Previous attempts to prepare the analogous Zr-bis-phosphinimide species such as $Zr(NPt\text{-}Bu_3)_2Cl_2$, **13**, from reaction of the Li-phosphinimide salts with $ZrCl_4$ resulted only in the isolation of the tris-substituted species $Zr(NPt\text{-}Bu_3)_3Cl$, **14**.[26] However, the synthesis of $Zr(NPt\text{-}Bu_3)_2(NEt_2)_2$, **12**, was achieved in 93% yield upon thermolysis of $Zr(NEt_2)_4$ with 2 equiv of $HNPt\text{-}Bu_3$ (Scheme 2). The formulation of **12** was confirmed by NMR spectroscopy as well as X-ray data (Figure 4). The Zr−phosphinimide-N distances of 1.988(12) and 2.029(15) Å were shorter than those determined for the amide ligands (2.042(16), 2.076(17) Å). Again, the phosphinimide groups were approximately linear at N, while the amido-N atoms exhibited a trigonal planar geometry. The angle between the phosphinimide groups at Zr was 115.6(7)°. This compares to the corresponding angles of

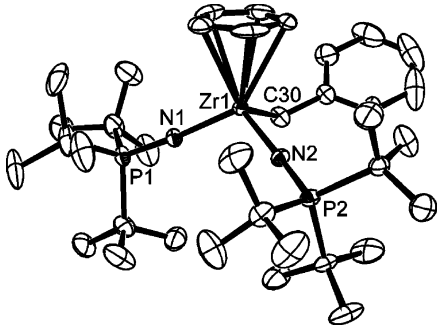

Figure 3. ORTEP drawing of **11**, with 30% thermal ellipsoids. Hydrogen atoms are omitted for clarity. Distances (Å) angles (deg): Zr(1)−N(2) 1.985(2), Zr(1)−N(1) 1.989(3), Zr(1)−C(30) 2.322(3), P(1)−N(1) 1.567(3), P(2)−N(2) 1.580(3), N(2)−Zr(1)−N(1) 110.83(10), N(2)−Zr(1)−C(30) 103.24(12), N(1)−Zr(1)−C(30) 97.26(12), P(1)−N(1)−Zr(1) 174.87(16), P(2)−N(2)−Zr(1) 173.84(16).

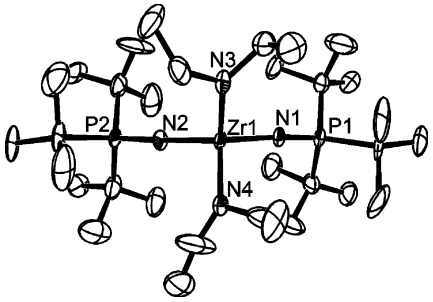

Figure 4. ORTEP drawings of **12**, with 30% thermal ellipsoids. Hydrogen atoms are omitted for clarity. Distances (Å) angles (deg): Zr(1)−N(1) 2.005(6), Zr(1)−N(2) 2.020(5), Zr(1)−N(3) 2.022(6), Zr(1)−N(4) 2.068(6), P(1)−N(1) 1.553(6), P(2)−N(2) 1.552(5), P(3)−N(3) 1.547(6), N(1)−Zr(1)−N(2) 110.3(2), N(1)−Zr(1)−N(3) 113.3(2), N(2)−Zr(1)−N(3) 112.4(2), N(1)−Zr(1)−N(4) 106.5(2), N(2)−Zr(1)−N(4) 107.8(2), N(3)−Zr(1)−N(4) 106.1(2), P(1)−N(1)−Zr(1) 171.1(4), P(2)−N(2)−Zr(1) 170.1(4), P(3)−N(3)−Zr(1) 176.2(4).

Scheme 2

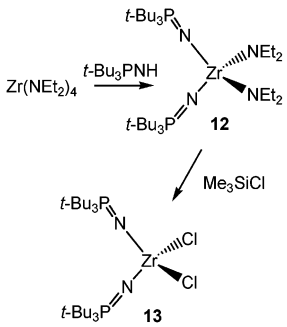

112.9(2)° and 117.24(11)° found in $Ti(NPt\text{-}Bu_3)_2Cl_2$ and $Ti(NPt\text{-}Bu_3)_2Me_2$, respectively.[13] The angle between the amido groups in **12** was smaller (106.6(7)°), presumably reflecting the lesser steric demands of the amido groups relative to the phosphinimide ligands. Subsequent reaction of **12** with Me_3SiCl afforded the species $Zr(NPt\text{-}Bu_3)_2Cl_2$, **13**, in 81% isolated yield. Attempts to alkylate **13** to give $Zr(NPt\text{-}Bu_3)_2Me_2$ using a number of methods were unsuccessful, affording a complex mixture of unresolved compounds.

In a method similar to that employed to obtain **12**, a transamination strategy was employed in efforts to prepare tris-substituted products. However, such efforts

(20) Giesbrecht, G. R.; Whitener, G. D.; Arnold, J. *Organometallics* **2000**, *19*, 2809−2812.
(21) Latesky, S. L.; McMullen, A. K.; Niccolai, G. P.; Rothwell, I. P. *Organometallics* **1985**, *4*, 902−908.
(22) Rogers, J. S.; Lachicotte, R. J.; Bazan, G. C. *Organometallics* **1999**, *18*, 3976−3980.
(23) Ciruelo, G.; Cuenca, T.; Gomez, R.; Gomez-Sal, P.; Martin, A.; Rodriguez, G.; Royo, P. *J. Organomet. Chem.* **1997**, *547*, 287−296.
(24) Tedesco, C.; Immirzi, A.; Proto, A. *Acta Crystallogr., Sect. B* **1998**, *B54*, 431−437.
(25) Swenson, D. C.; Guo, Z.; Crowther, D. J.; Baenziger, N. C.; Jordan, R. F. *Acta Crystallogr. C* **2000**, *C56*, e313−e314.
(26) Guerin, F.; Stewart, J. C.; Beddie, C.; Stephan, D. W. *Organometallics* **2000**, *19*, 2994−3000.

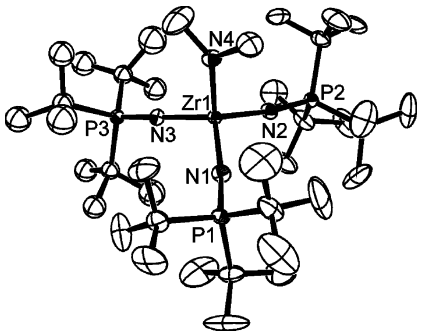

Figure 5. ORTEP drawings of **15**, with 30% thermal ellipsoids. Hydrogen atoms are omitted for clarity. Distances (Å) angles (deg): Zr(1)−N(2) 1.988(12), Zr(1)−N(1) 2.029(15), Zr(1)−N(3) 2.042(16), Zr(1)−N(4) 2.076(17), P(1)−N(1) 1.540(16), P(2)−N(2) 1.596(13), N(2)−Zr(1)−N(1) 115.6(7), N(2)−Zr(1)−N(3) 110.7(6), N(1)−Zr(1)−N(3) 107.4(6), N(2)−Zr(1)−N(4) 106.7(6), N(1)−Zr(1)−N(4) 109.4(6), N(3)−Zr(1)−N(4) 106.6(7), P(1)−N(1)−Zr(1) 175.4(9), P(2)−N(2)−Zr(1) 178.0(10).

gave mixtures of inseparable products. In the case of $Zr(NPt\text{-}Bu_3)_3(NMe_2)$, **15**, this compound was obtained in less than 5% yield using this synthetic method. However, **15** was obtained cleanly and directly from the ligand metathesis reaction of $Zr(NPt\text{-}Bu_3)_3Cl$, **14**, with $LiNMe_2$. X-ray analysis of **15** (Figure 5) confirmed the formulation and revealed approximately linear Zr−phosphinimide linkages. The Zr−N distances in **15** varied from 2.005(6) to 2.022(6) Å, while the Zr−amide distance was longer, at 2.068(6) Å. The slightly longer Zr−phosphinimide bonds resulted in slightly smaller P−N distances of 1.553(6), 1.552(5), and 1.547(6) Å, which are shorter than that seen for related Cp analogues.

Cations and Zwitterions. We have previously reported that reaction of **4** with $B(C_6F_5)_3$ resulted in the immediate formation of $CpZr(NPt\text{-}Bu_3)(C_6F_5)_2$. This was independently confirmed via its preparation from **2** and the Grignard reagent C_6F_5MgBr.[16] However, we have since discovered that methyl for C_6F_5 exchange was prevented when **4** was reacted with $B(C_6F_5)_3$ in the presence of donors (Scheme 3). For example, in the presence of THF, the salt $[CpZr(NPt\text{-}Bu_3)Me(THF)][MeB(C_6F_5)_3]$, **16**, was isolated. This cation is analogous to those previously described for analogues based on zirconocene and constrained geometry catalysts.[27−31]

Similarly, reaction of **3** or **4** with $B(C_6F_5)_3$ in the presence of the carbodiimide $(i\text{-}PrN)_2C$ afforded insertion into the Zr−Me bond, providing $[Cp^*Zr(NPt\text{-}Bu_3)((i\text{-}PrN)_2CMe)][MeB(C_6F_5)_3]$, **17**, and $[CpZr(NPt\text{-}Bu_3)((i\text{-}PrN)_2CMe)][MeB(C_6F_5)_3]$, **18**, respectively. In each of the species **16**−**18**, the B-bound methyl group gave rise to a broad proton signal at ∼0.5 ppm and a broad quartet in the $^{13}C\{^1H\}$ NMR spectra at ∼10 ppm with $^1J_{B-C}$ values of 20−50 Hz. Similarly, reaction of $[HNMe_2Ph][B(C_6F_5)_4]$ with **4** generated the salt $[CpZr(NPt\text{-}Bu_3)Me(NMe_2Ph)][B(C_6F_5)_4]$, **19**, which was stabilized by the amine liberated by protonolysis. In general, the salts above were difficult to isolate, as they were generally unstable in solution. Only **17** and **18** could be isolated in an analytically pure form, since they are stable in CH_2Cl_2 solution under an inert atmosphere for up to 6 months. Related recent reports have described the synthesis and characterization of neutral Zr amidinate and cationic Zr guanidinate complexes.[32−35]

Increased steric protection at Zr permitted the generation of an apparently base-free cation. Reaction of **11** with $B(C_6F_5)_3$ gave the species formulated as $[CpZr(NPt\text{-}Bu_3)_2][BnB(C_6F_5)_3]$, **20**. The methylene protons gave rise to a broadened signal in the ^1H NMR spectrum, and the ^{11}B NMR signal of −16.6 ppm confirmed a tetracoordinate boron anion. The absence of crystallographic data or conclusive spectroscopic data precluded clarification on the nature of the cation−anion interaction in **20**, although previous work has described related zwitterionic complexes with interactions between the borate-bound benzyl group and the cationic center.[36−39]

The synthesis and characterization of the zwitterionic species and salts above demonstrate that cationic Zr-phosphinimide species are accessible. This suggests that effective polymerization catalysts from Zr-phosphinimide species should be accessible. These reactivity studies stand in contrast to earlier efforts that suggested C−H activation and methyl for C_6F_5 exchange deactivation pathways might preclude effective olefin polymerization by Zr-phosphinimide-based catalysts.[16]

Steric Bulk and Molecular Orbital Considerations. The initial premise for use of bulky phosphinimide ligands in the design of olefin polymerization catalysts was the notion that the phosphinimide ligand would occupy a cone of space similar to that occupied by a cyclopentadienyl ligand.[14,15] The structural data above suggest that is the case. On the basis of these data, the cone angles for the cyclopentadienyl and $t\text{-}Bu_3$-PN ligands on Zr are estimated to be 82° and 88°, respectively. While these ligands occupy similar volumes, the key difference is that the majority of the steric bulk of the phosphinimide is located further away from the metal center. Thus, though a phosphinimide ligand may offer similar steric protection to a Cp ligand in terms of second-sphere interactions, the phosphinimide ligand offers an environment that is more open in the vicinity of the metal center, a feature that may be responsible for enhanced polymerization activity.

Previous authors have considered the electronic similarity of Cp−M and R_3PN−M interactions.[40] Herein,

(27) Deck, P. A.; Beswick, C. L.; Marks, T. *J. Am. Chem. Soc.* **1998**, *120*, 1772−1784.
(28) Yang, X.; Stern, C. L.; Marks, T. J. *J. Am. Chem. Soc.* **1991**, *113*, 3623−3625.
(29) Yang, X.; Stern, C.; Marks, T. *J. Am. Chem. Soc.* **1994**, *116*, 10015−10031.
(30) Guo, Z.; Swenson, D. C.; Jordan, R. F. *Organometallics* **1994**, *13*, 1424−1432.
(31) Oberhoff, M.; Erker, G.; Frohlich, R. *Chem.−Eur. J.* **1997**, *3*, 1521−1525.
(32) Littke, A.; Sleiman, N.; Bensimon, C.; Richeson, D. S.; Yap, G. P. A.; Brown, S. J. *Organometallics* **1998**, *17*, 446−451.
(33) Ong, T.-G.; Yap, G. P. A.; Richeson, D. S. *Organometallics* **2003**, *22*, 387−389.
(34) Ong, T.-G.; Wood, D.; Yap, G. P. A.; Richeson, D. S. *Organometallics* **2002**, *21*, 1−3.
(35) Wood, D.; Yap, G. P. A.; Richeson, D. S. *Inorg. Chem.* **1999**, *38*, 5788−5794.
(36) Bochmann, M.; Lancaster, S. J. *Organometallics* **1993**, *12*, 633−640.
(37) Bochmann, M.; Lancaster, S. J. *Makromol. Chem.* **1993**, *14*, 807−811.
(38) Chen, Y.-X.; Fu, P.-F.; Stern, C. L.; Marks, T. J. *Organometallics* **1997**, *16*, 5958−5963.
(39) Amor, J. I.; Cuenca, T.; Galakhov, M.; Gomez-Sal, P.; Manzanero, A.; Royo, P. *J. Organomet. Chem.* **1997**, *535*, 155−168.
(40) Dehnicke, K.; Krieger, M.; Massa, W. *Coord. Chem. Rev.* **1999**, *182*, 19−65.

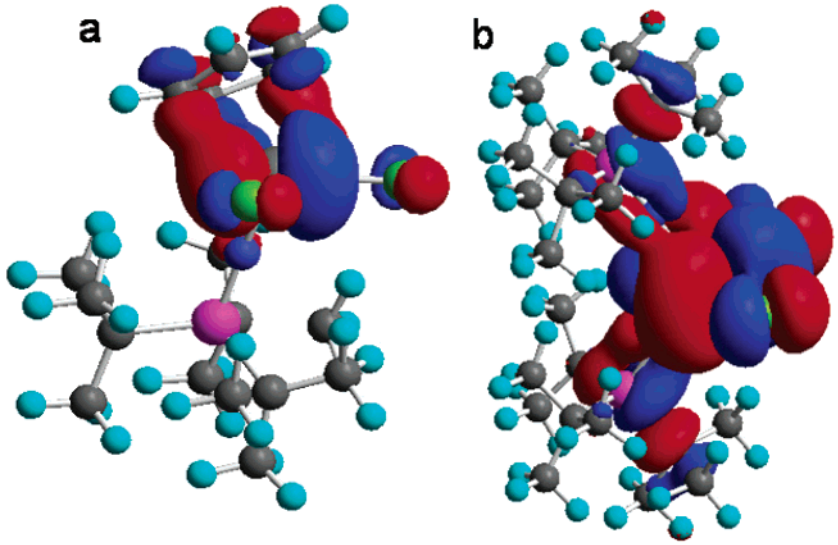

Figure 6. Plots of LUMOs of CpZr(NP*t*-Bu$_3$)Cl$_2$ (left) and Zr(NP*t*-Bu$_3$)$_2$Cl$_2$ (right) based on static DFT calculations.

Scheme 3

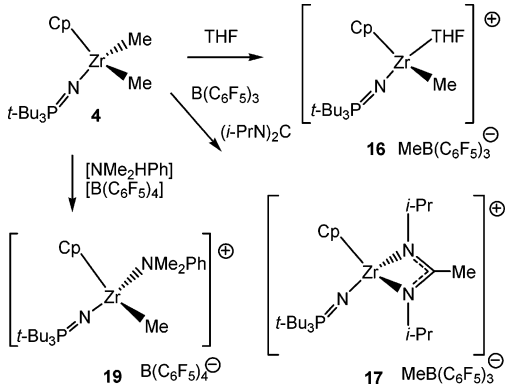

single-point Gaussian calculations using the Hartree−Fock method and STO-3g basis set were done on the molecules CpZr(NP*t*-Bu$_3$)Cl$_2$ and Zr(NP*t*-Bu$_3$)$_2$Cl$_2$ using the structural parameters derived and modified from the crystallographic data. In the case of CpZr(NP*t*-Bu$_3$)-Cl$_2$, the HOMO, HOMO-1, and HOMO-2 orbitals all are comprised of significant N−Zr interactions, consistent with σ and π bonding between Zr and N. Calculations for the bis-phosphinimide system show similar Zr−N interactions. These observations are consistent with the view that sterically demanding substituents on P preclude interaction of these HOMOs with sterically unencumbered Lewis acids. This view is also supported by our recent work in which Ti-phosphinimide derivatives reacted with AlMe$_3$ via interaction of Al with the phosphinimide N atom to effect C−H activation.[41−44] The LUMOs in both cases are comprised primarily of Zr-based d-orbitals. These orbitals are of symmetry similar to that of the 1a$_1$ orbital described in the classic extended Huckel description for bent metallocenes, suggesting that CpZr-phosphinimide or Zr-bis-phosphinimide derivatives are electronically similar to zirconocenes, suggesting the possibility of effective olefin polymerization activity.

Ethylene Polymerization. Screening of **1**−**4** using MAO as a solvent scrubber/activator resulted in moderate polymerization activities relative to zirconocene standards and analogous Ti-precursors (Table 2). As a possible explanation, it is worth considering that previous reports have demonstrated that Zr-phosphinimide precursors react with trialkylaluminum reagents.[16] It is noteworthy that the polymer produced from **2**/MAO was similar to that derived from CpZrCl$_3$/MAO (i.e., low molecular weight and high PDI), suggesting that ligand abstraction may be involved in the catalyst degradation process. This view is consistent with reactivity studies of Zr-phosphinimide complexes with AlMe$_3$ to afford clusters that have no phosphinimide ligands present. Additional bulk on the cyclopentadienyl ligand in Cp*Zr-(NP*t*-Bu$_3$)Cl$_2$ resulted in two distinct polymer products. There is a lower molecular weight fraction (M_n = 3070) reminiscent of that produced from **2**/MAO, as well as a higher molecular weight fraction (M_n = 783 900). These data suggest the presence of two catalysts: one that originates from the activation of the half-sandwich phosphinimide precursor, and the other from a ligand-abstraction product.

In an effort to achieve higher polymerization activities, the method of activation was modified. Twenty equivalents of Al(*i*-Bu)$_3$ and 2 equiv of B(C$_6$F$_5$)$_3$ or [Ph$_3$C][B(C$_6$F$_5$)$_4$] were used as scavenger and cocatalyst, respectively. This activation strategy employed with the catalyst precursors **3**, **4**, and **6** resulted in a significant increase in activity relative to MAO activation. Interestingly, the activity derived from **4** was slightly greater than that seen for the catalysts derived from **3**. Another interesting result is that the use of **6** as a catalyst precursor with the cocatalyst B(C$_6$F$_5$)$_3$ resulted in a polymerization activity that is approximately double that derived from **4**. This may be attributed to an anion effect similar to that previously described by Bochmann and co-workers.[45] Efforts to characterize the zwitterion derived from the reaction of **6** and B(C$_6$F$_5$)$_3$ resulted in intractable mixtures of products, although it should be

(41) Kickham, J. E.; Guerin, F.; Stephan, D. W. *J. Am. Chem. Soc.* **2002**, *124*, 11486−11494.
(42) Kickham, J. E.; Guerin, F.; Stewart, J. C.; Urbanska, E.; Ong, C. M.; Stephan, D. W. *Organometallics* **2001**, *20*, 1175−1182.
(43) Kickham, J. E.; Guerin, F.; Stewart, J. C.; Urbanska, E.; Ong, C. M.; Stephan, D. W. *Organometallics* **2001**, *20*, 3209.
(44) Kickham, J. E.; Guerin, F.; Stewart, J. C.; Stephan, D. W. *Angew. Chem., Int. Ed.* **2000**, *39*, 3263−3266.
(45) Zhou, J.; Lancaster, S. J.; Walker, D. A.; Beck, S.; Thornton-Pett, M.; Bochmann, M. *J. Am. Chem. Soc.* **2001**, *123*, 223−237.

Table 1. Crystallographic Data[a]

	1	**8**	**6**	**11**	**12**	**15**
formula	$C_{22}H_{42}Cl_2NPZr$	$C_{22}H_{37}ClNPZr$	$C_{31}H_{46}NPZr$	$C_{36}H_{66}N_2P_2Zr$	$C_{32}H_{72}N_4P_2Zr$	$C_{38}H_{60}N_4P_3Zr$
fw	513.66	473.17	554.88	680.07	666.10	757.03
a (Å)	11.888(6)	8.472(4)	11.354(6)	10.759(6)	17.789(17)	13.306(9)
b (Å)	16.743(9)	14.295(7)	15.765(8)	19.554(12)	17.802(17)	13.409(9)
c (Å)	13.508(7)	19.506(9)	16.780(9)	19.429(12)	25.81(3)	16.000(11)
α (deg)						79.100(13)
β (deg)	96.934(9)			103.548(12)		73.208(12)
γ (deg)						60.701(13)
cryst syst	monoclinic	orthorhombic	orthorhombic	monoclinic	orthorhombic	triclinic
V (Å^3)	2669(2)	2362(2)	3004(3)	3974(4)	8175(14)	2379(3)
space group	*P*2(1)/*n*	*P*2(1)2(1)2(1)	*P*2(1)2(1)2(1)	*P*2(1)/*c*	*Pbca*	$P\bar{1}$
δ(calc) (g cm^{-1})	1.278	1.330	1.227	1.137	1.082	1.057
Z	4	4	4	4	8	2
abs coeff, μ (cm^{-1})	0.680	0.653	0.437	0.381	0.370	0.357
no. of data collected	11 059	10 186	12 830	16 934	23 352	9774
no. of data $F_o^2 > 3\sigma(F_o^2)$	3807	3372	4279	5720	4076	6723
no. of variables	244	235	307*	370	352	379
R	0.0249	0.0493	0.0217	0.0339	0.1074	0.0722
R_w	0.0694	0.1288	0.0560	0.0850	0.2386	0.1864
GOF	1.025	1.018	1.031	0.872	0.982	1.187

[a] All data collected at 24 °C with Mo Kα radiation (λ = 0.71069 Å), $R = \sum||F_o| - |F_c||/\sum|F_o|$, $R_w = [\sum[w(F_o^2 - F_c^2)^2]/\sum[wF_o^2)^2]]^{0.5}$.

Table 2. Ethylene Polymerization Data[a]

precat.	cocat.	act.[e]	M_n	M_w	PDI	precat.	cocat.	act.[e]	M_n	M_w	PDI
1	MAO	170	3070	5930	1.9	**3**	$B(C_6F_5)_3$	270	59 900	161 300	2.7
			783 900	1 261 000	1.6						
2	MAO	100	3450	234 300	67.9	**4**	$B(C_6F_5)_3$	400	6640	94 900	14.3
3	MAO	70				**6**	$B(C_6F_5)_3$	850			
4	MAO	90	36 500	94 300	2.6	Cp_2ZrMe_2	$B(C_6F_5)_3$	1760	69 500	192 300	2.8
$CpZrCl_3$	MAO	10	9480	313 600	33.1	**3**	$[Ph_3C][B(C_6F_5)_4]$	1010	54 200	177 000	3.3
Cp_2ZrCl_2	MAO	600	161 100	340 800	2.1	**4**	$[Ph_3C][B(C_6F_5)_4]$	1270	7450	24 400	3.3
Cp_2ZrMe_2	MAO	866	99 400	221 200	2.2	**6**	$[Ph_3C][B(C_6F_5)_4]$	1040			
12	MAO[b]	*c*	*c*	*c*	*c*	Cp_2ZrMe_2	$[Ph_3C][B(C_6F_5)_4]$	1030	171 000	334 800	1.9
13	MAO[b]	60	18 300	197 000	10.8						
Cp_2ZrCl_2	MAO[b]	2030	95 100	293 300	3.1						
Cp_2ZrMe_2	MAO[b]	1880	78 200	201 500	2.6						

[a] Toluene, 30 °C, 1.82 atm C_2, 50 μM precatalyst, 30 min; MAO activation Zr:Al ratio 1:500; $B(C_6F_5)_3$ or $Ph_3CB(C_6F_5)_4$ activation: Zr:Al ratio 1:20 (T*i*-BAl), 10 min. [b] 10 min. [c] Too little polymer to analyze. [d] 2.5 min after *T* spiked to 73 °C. [e] Activity reported in g mmol^{-1} h^{-1} atm^{-1}.

noted that, in contrast to **2**, no evidence for the formation of $CpZr(NPt\text{-}Bu_3)(C_6F_5)_2$ was observed. With all precatalysts, use of $[Ph_3C][B(C_6F_5)_4]$ as the cocatalyst led to significantly higher polymerization activities (Table 2). These results were achieved in the presence of higher ethylene pressures (1.82 atm) than previously employed (1 atm),[16] implying that these Zr catalysts may be prone to deactivation in the absence of sufficient ethylene supply. Reaction of the bis-phosphinimide species **13** with MAO as an activator gave only moderate activity (Table 2), in contrast to the extremely active Ti-bis-phosphinimide catalysts.[13]

Summary

Synthetic routes to Zr-phosphinimide complexes have been developed. Subsequently, corresponding salts have been formed by reaction of suitable precursors with various Lewis acids in the presence of stabilizing donor ligands. These molecules have demonstrated steric and electronic simliarities to analogous zirconocene-based precursors, generating ethylene polymerization catalysts whose activities vary considerably depending on the activation strategy. Activation by MAO provided generally low polymerization activity, while higher activities were derived from use of $B(C_6F_5)_3$ or $[Ph_3C][B(C_6F_5)_4]$ in the presence of low concentrations of Al(*i*-Bu)$_3$ as a scavenger and higher ethylene supply pressure.

Acknowledgment. Financial support from NSERC of Canada and NOVA Chemicals Corporation is gratefully acknowledged. E.H. is grateful for the award of an Ontario Graduate Scholarship.

Supporting Information Available: Crystallographic data in CIF format are deposited on-line. NMR data for compounds **16**, **19**, and **20** are deposited. This material is available free of charge via the Internet at http://pubs.acs.org.

OM030631C